doi: 10.1038/nature06977

Supplementary Information

Modest stabilization by most hydrogen-bonded side-chain interactions in membrane proteins

Nathan HyunJoong Joh[1], Andrew Min[1], Salem Faham[2], Julian P. Whitelegge[3], Duan Yang[1], Virgil L. Woods Jr.[4] & James U. Bowie[1]

[1]Department of Chemistry and Biochemistry, UCLA-DOE Center for Genomics and Proteomics, Molecular Biology Institute, [2]Department of Physiology, [3]The NPI-Semel Institute, Pasarow Mass Spec Laboratory, University of California, Los Angeles, CA 90095

[4]Department of Medicine and Biomedical Sciences Graduate Program, University of California, San Diego, La Jolla, CA 92093-0656

Supplementary Methods

Double Mutant Cycle Analysis and Unfolded State Effects. It is often assumed that the double mutant cycle can not compensate for unfolded state effects[1]. This is not the case, however. A double mutant cycle is illustrated in the diagram below. We would like to measure the interaction free energy ΔG_{xy} between residues X and Y. All the equilibria shown are between *folded* states, but we can't measure that directly so we use the expedient of measuring unfolding free energies. If we delete residue Y, we delete the interaction, ΔGxy and anything else that Y does, ΔG_{Yother}. This equilibrium is measured by comparing unfolding free energies between the wild-type, ΔGu^{WT}, and the mutant ΔGu^{Y} ($\Delta\Delta Gu = \Delta G_{xy} + \Delta G_{Yother} = \Delta Gu^{Y} - \Delta Gu^{WT}$). Thus ΔG_{Yother} is any additional energetic contribution made in the folded *or* unfolded states. Similarly, when we knock out residue X, we delete the interaction, ΔG_{xy} and anything else that X does in the folded or unfolded states. So if we sum the $\Delta\Delta Gu$ for the single mutants and subtract the $\Delta\Delta Gu$ for the double mutant, we eliminate free energy contributions due to new interactions in the unfolded state as long as they are additive and independent and that the interaction is broken in the unfolded state.

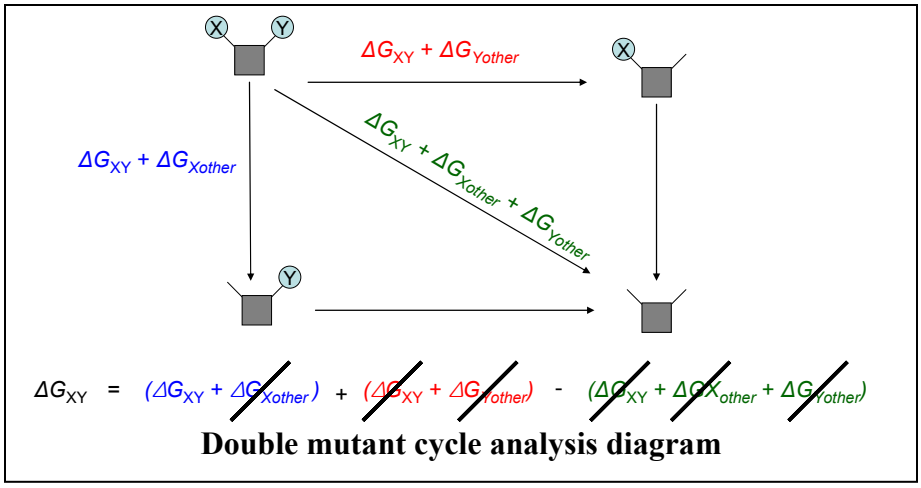

Double mutant cycle analysis diagram

Do the native tertiary hydrogen bonds between side chains break in the SDS unfolded state? We can not know for certain, but the available evidence suggests that most of the native, long range hydrogen bonds between side chains are broken in the SDS unfolded state. bR migrates normally in SDS-PAGE suggesting the lack of stable structure. NMR studies of a fragment of bR consisting of helices A and B show no tertiary NOEs in SDS suggesting that the interaction between helices A and B is minimal in SDS[2]. Moreover, helices A and B do not make stable interactions with the rest of the protein in SDS[3]. Finally, hydrogen exchange rates increase in SDS relative to bicelles for all peptide regions we have monitored indicating increased penetration of water throughout the protein (unpublished).

Supplementary Table 1. Thermodynamic parameters of detergent-induced unfolding and the interaction free energies estimated from double-mutant cycles.

Interaction	bR variant	Cm [a] (X_{SDS})	m [b] (kcal mol^{-1} X_{SDS}^{-1})	$\Delta\Delta G_{unfolding}$ [c] (kcal mol^{-1})
	WT	0.60	– 23.9 ± 0.9	0.0 ± 0.2
K30 – Y43	K30M	0.61	– 20.8 ± 0.8	0.3 ± 0.1
	Y43F	0.60	– 24 ± 1	0.1 ± 0.2
	K30M/Y43F	0.63	– 18.1 ± 0.5	0.6 ± 0.2
				$\Delta G_{int.}$ = – 0.1 ± 0.3 kcal mol^{-1}
T46 – D96	T46A	0.51	– 20.6 ± 0.9	– 1.8 ± 0.2
	D96A	0.53	– 24 ± 2	– 1.5 ± 0.1
	T46A/D96A	0.52	– 21.5 ± 0.3	– 1.6 ± 0.2
				$\Delta G_{int.}$ = – 1.7 ± 0.3 kcal mol^{-1}
Y79 – E9	Y79F	0.59	– 24 ± 1	– 0.1 ± 0.1
	E9A	0.59	– 21 ± 2	– 0.1 ± 0.1
	Y79F/E9A	0.60	– 20.3 ± 0.7	– 0.1 ± 0.2
				$\Delta G_{int.}$ = – 0.1 ± 0.2 kcal mol^{-1}
T90 – D115	T90A	0.54	– 25 ± 1	– 1.3 ± 0.1
	D115A	0.62	– 22.1 ± 0.6	0.5 ± 0.1
	T90A/D115A	0.66	– 16 ± 1	0.9 ± 0.2
				$\Delta G_{int.}$ = – 1.7 ± 0.3 kcal mol^{-1}
T170 – S226	T170A	0.57	– 29.5 ± 0.4	– 0.9 ± 0.2
	S226A	0.55	– 19.7 ± 0.7	– 0.9 ± 0.1
	T170A/S226A	0.54	– 15.9 ± 0.2	– 1.0 ± 0.2
				$\Delta G_{int.}$ = – 0.8 ± 0.3 kcal mol^{-1}
Y185 – D212	Y185F	0.58	– 22.5 ± 0.3	– 0.4 ± 0.2
	D212A	0.49	– 12 ± 3	– 1.2 ± 0.3
	Y185F/D212A	0.50	– 12.6 ± 0.4	– 1.2 ± 0.2
				$\Delta G_{int.}$ = – 0.4 ± 0.4 kcal mol^{-1}
W189 – Y83	W189F	0.64	– 24.1 ± 0.8	1.0 ± 0.1
	Y83F	0.60	– 23 ± 1	0.1 ± 0.1
	W189F/Y83F	0.63	– 18.7 ± 0.5	0.7 ± 0.1
				$\Delta G_{int.}$ = 0.4 ± 0.2 kcal mol^{-1}
S193 – E204	S193A	0.60	– 22.6 ± 0.6	0.1 ± 0.1
	E204A	0.51	– 18 ± 4	– 1.5 ± 0.1
	S193A/E204A	0.54	– 15 ± 1	– 0.9 ± 0.2
				$\Delta G_{int.}$ = – 0.5 ± 0.3 kcal mol^{-1}

[a] SDS mole fraction at the midpoint of the transition

[b] Dependence of the free energy of unfolding on SDS mole fraction. We do not know the origin of the changes in m-values we observed for the mutants. The stability comparisons are performed where the wild-type protein is 50% unfolded so that most free energy measurements are made within the transition zones where the fraction unfolded can be directly measured or involved minimal extrapolation.

[c] Change in stability from wild-type at the wild-type C_m

Supplementary Table 2. X-ray data collection and refinement statistics.

	bR D115A	bR T90A/D115A
Data Collection*		
Wavelength (Å)	1.1271	1.0000
Space Group	$P2_1$	$P2_1$
Cell Dimensions		
a, b, c (Å)	45.4, 109.0, 56.4	44.0, 109.7, 55.5
α, β, γ (°)	90, 113.7, 90	90, 113.4, 90
Resolution (Å)	90.0 - 2.30 (2.38 - 2.30)	40.0 - 2.70 (2.80 - 2.70)
R_{sym}	0.130 (0.365)	0.134 (0.219)
$I/\sigma I$	8.1 (2.9)	6.2 (3.1)
Completeness (%)	93.8 (84.0)	91.0 (65.1)
Redundancy	3.0 (2.3)	2.8 (2.2)
Refinement**		
Resolution (Å)	29.71 - 2.31	29.70 - 2.70
No. Reflections	19,599	11,592
R_{work} / R_{free}	0.221 / 0.275	0.273 / 0.287
No. Atoms		
Protein	3,508	3,504
Ligand/ion	40	40
Water	134	38
B-factors		
Protein	20.5	33.6
Ligand / ion	16.5	27.6
Water	25.6	18.8
r.m.s Deviation		
Bond Lengths (Å)	0.007	0.005
Bond Angles (°)	1.1	1.0
Ramachandran Stats (%)		
Core	96.4	96.9
Allowed Region	3.6	3.1
Gen. Allowed Region	0.0	0.0
Disallowed Region	0.0	0.0

* A set of data collected from one crystal was used to refine each of bR D115A and bR T90A/D115A structure. Data from bR D115A and bR T90A/D115A were collected at the beamline 8.2.2 and 8.2.1, respectively, under cryogenic condition. Values in the parentheses are for the last resolution shell.

** Twinning operation ($-h, -k, h + l$) was performed in reciprocal space during structure refinement.

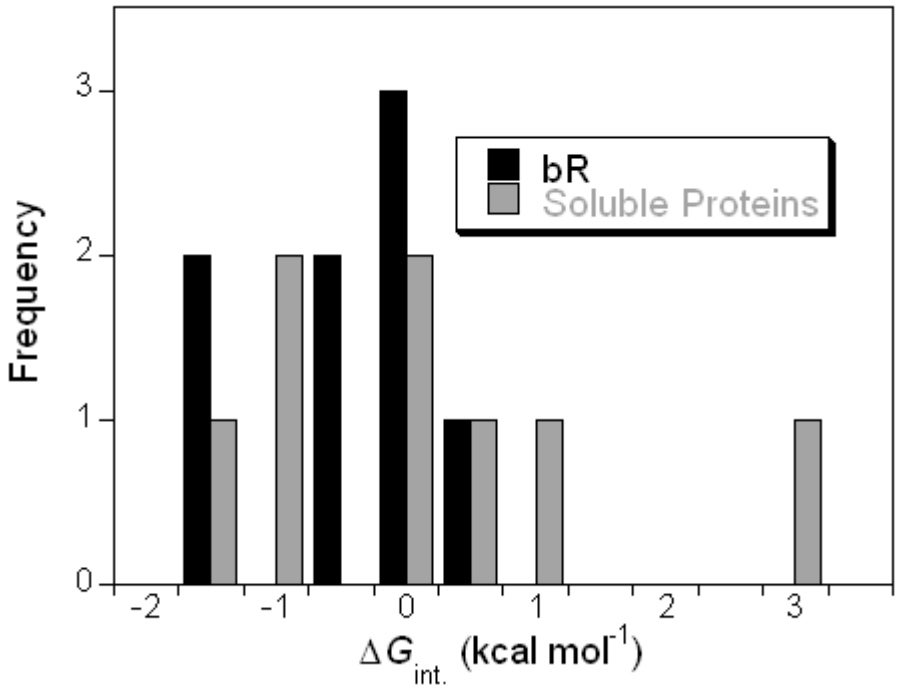

Supplementary Figure 1 | Comparison of pair-wise side-chain interaction strengths of hydrogen bonding residues in bacteriorhodopsin and soluble proteins. The strengths of hydrogen bonding side-chain interactions in soluble proteins estimated by double-mutant cycle analysis[4-7] in literatures are compared with the present hydrogen bonding side-chain interaction free energies in bacteriorhodopsin.

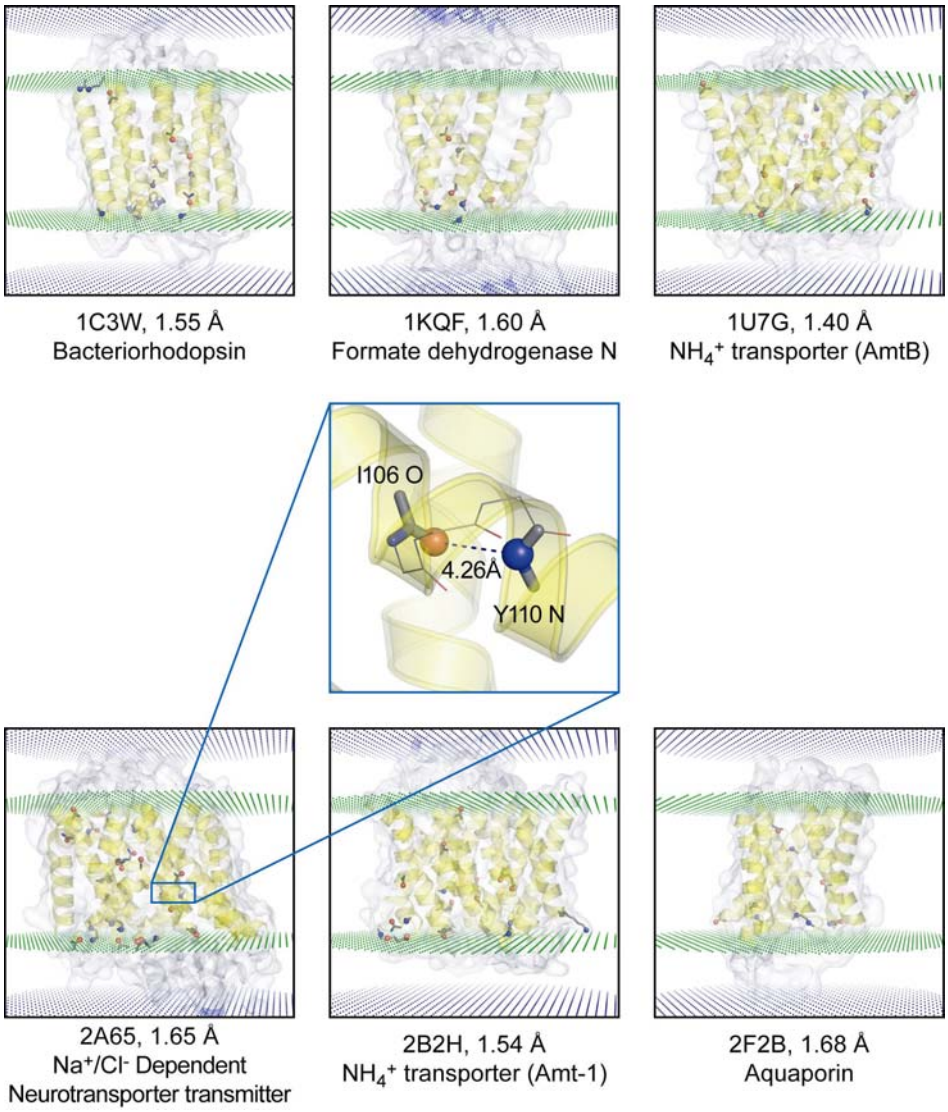

Supplementary Figure 2 | Uncoordinated hydrogen bond donors and acceptors in the hydrophobic cores of membrane proteins. HBPLUS software was used to identify unsatisfied hydrogen bonded donors and acceptors in the hydrophobic cores of six unique membrane protein structures solved at 1.7 Å or better. The proteins are shown in cartoons with the approximate hydrocarbon core, the interfacial and aqueous exposed regions of the bilayer environment highlighted in yellow, white and blue respectively. Uncoordinated donors and acceptors are shown as spheres and neighboring atoms covalently bonded to the uncoordinated donors and acceptors are shown as sticks. For clarity, hydrophobic cores are separated by a plane of green dots and interfacial regions are separated from water environment by blue dots. A close-up view of an example of uncoordinated donor and acceptor, Y110 N and I106 O, respectively, from Na^+/Cl^- dependent neurotransporter transmitter (PDB ID: 2A65) is shown in the center.

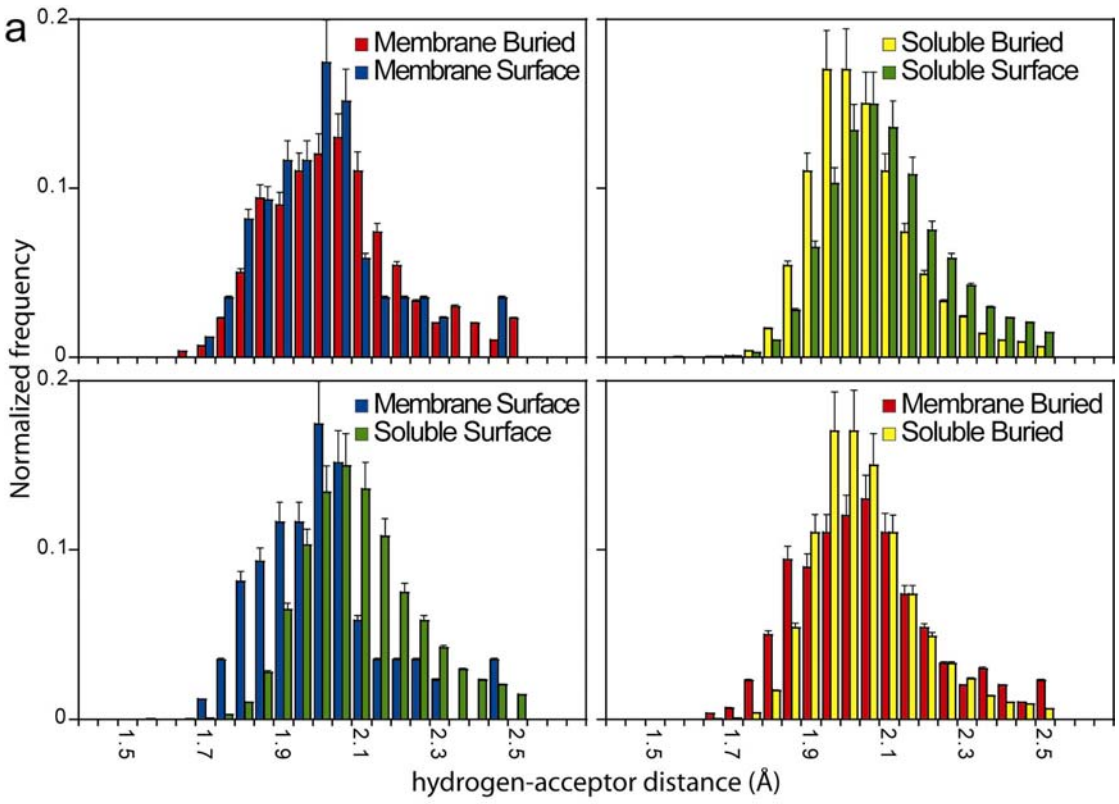

b

	Membrane Buried vs. Membrane Surface		Soluble Buried vs. Soluble Surface	
N	299	86	11235	11366
<x>	2.02 ± 0.17	1.98 ± 0.16	2.02 ± 0.13	2.08 ± 0.15
P	0.038		5.7×10^{-204}	

	Membrane Surface vs. Soluble Surface		Membrane Buried vs. Soluble Surface	
N	86	11366	299	11235
<x>	1.98 ± 0.16	2.08 ± 0.15	2.02 ± 0.17	2.02 ± 0.13
P	1.8×10^{-7}		0.80	

Supplementary Figure 3 | Comparison of hydrogen-acceptor distance distributions of α-helix backbone-backbone hydrogen bonds in soluble proteins and in the hydrocarbon core embedded region of membrane proteins. **a,** Normalized hydrogen-acceptor distance distributions of buried residues in hydrocarbon core of membrane proteins (Membrane Buried, shown in blue), on surface of hydrocarbon core of membrane proteins (Membrane Surface, shown in red), buried in soluble proteins (Soluble Buried, shown in green) and on the surface of soluble proteins (Soluble Surface, shown in yellow) are plotted as histograms for pair-wise comparison. Error bars were estimated using N indicated in **b**, assuming that the distributions are multinomial. **b,** The results from statistical analysis of each distribution comparison shown in A are tabulated, where N is population size, <x> is mean hydrogen-acceptor distance ± standard deviation, and P is the probability that the two means are different by random chance.

1. Fersht AR, Matouschek A, Serrano L. The folding of an enzyme. I. Theory of protein engineering analysis of stability and pathway of protein folding. *J. Mol. Biol.* **224**, 771–82 (1992)

2. Pervushin KV, Orekhov V, Popov AI, Musina L, Arseniev AS. Three-dimensional structure of (1-71)bacterioopsin solubilized in methanol/chloroform and SDS micelles determined by 15N-1H heteronuclear NMR spectroscopy. *Eur. J. Biochem.* **219**, 571–83 (1994)

3. Popot JL, Gerchman SE, Engelman DM. Refolding of bacteriorhodopsin in lipid bilayers. A thermodynamically controlled two-stage process. *J. Mol. Biol.* **198**, 655–76 (1987)

4. Marqusee S, Sauer RT. Contributions of a hydrogen bond/salt bridge network to the stability of secondary and tertiary structure in lambda repressor. *Protein Sci.* **3**, 2217–25 (1994)

5. Fernandez-Recio J, Romero A, Sancho J. Energetics of a hydrogen bond (charged and neutral) and of a cation-pi interaction in apoflavodoxin. *J. Mol. Biol.* **290**, 319–330 (1999)

6. Jang DS, Cha HJ, Cha SS, Hong BH, Ha NC, Lee JY, Oh BH, Lee HS, Choi KY. Structural double-mutant cycle analysis of a hydrogen bond network in ketosteroid isomerase from Pseudomonas putida biotype B. *Biochemical Journal* **382**, 967–973 (2004)

7. Campos LA, Cuesta-Lopez S, Lopez-Llano J, Falo F, Sancho J. A double-deletion method to quantifying incremental binding energies in proteins from experiment: Example of a destabilizing hydrogen bonding pair. *Biophys. J.* **88**, 1311–1321 (2005)